Journal of Fluorescence, Vol. 3, No. 3, 1993

Fluorescence Lifetime Imaging of Intracellular Calcium

Henryk Szmacinski,[1] Joseph R. Lakowicz,[1] W. J. Lederer[2], K. Nowaczyk,[1] and Michael L. Johnson[3]

Received October 18, 1993

Fluorescence lifetime imaging microscopy (FLIM) is a new methodology for studying the spatial and temporal dynamics of macromolecule, molecules, and ions in living cells. In FLIM image contrast is derived from the mean fluorescence lifetime at each point in a two-dimensional image. In our case the lifetime was measured by the phase-modulation method. We describe our FLIM apparatus, which consists of a fluorescence microscope, high-speed gated proximity focused MCP image intensifier, and slow-scan CCD camera. To accomplish subnanosecond time-resolved imaging, the gain of the image intensifier is modulated with a high-frequency signal, resulting in stationary phase-sensitive intensity images on the image intensifier. These images are recorded using a cooled slow-scan CCD camera and stored in an image processor. The lifetime images are created from a series of phase-sensitive images at various phase shift of the gain-modulation signal. We demonstrate calcium concentration imaging in living COS cells based on Ca^{2+}-induced lifetime changes of Quin-2. The phase-angle image is mapped to the Ca^{2+} concentration image using an *in vitro*-determined calibration curve. The Ca^{2+} concentration was found to be uniform throughout the cell. In contrast, the intensity image shows significant spatial differences, which likely reflect variations in the thickness and distribution of probe within the cell.

KEY WORDS: Fluorescence lifetime imaging microscopy; intracellular calcium; live cells.

INTRODUCTION

Currently, most fluorescence microscopic measurements are performed as steady-state measurements [1–6]. The steady-state fluorescence images can be difficult to interpret and quantify because there is no practical way to determine local concentration of the probes in various regions of the sample. Moreover, most fluorophores photobleach rapidly, which further complicates the ability to use the intensity images quantitatively. As a result of these difficulties, there have been extensive efforts to develop probes and imaging methods that are independent of the local intensity, such as the wavelength-ratiometric probes for Ca^{2+} and Mg^{2+}. However, in spite of extensive efforts, most currently useful ratiometric probes require UV excitation. Those probes that allow visible wavelength excitation, such as calcium green, magnesium green [7], and sodium green [8], do not display shifts of the excitation and/or emission wavelengths.

Recent advances in electronics, electrooptics, acoustooptics, and laser technology have now made possible a new type of imaging microscopy. Instead of fluorescence intensities or intensity ratios, it is now possible to measure the fluorescence lifetime at each point in the image, a technique we call fluorescence lifetime imaging microscopy (FLIM). Importantly, the use of lifetime im-

[1] Center for Fluorescence Spectroscopy, Department of Biological Chemistry, University of Maryland, School of Medicine, 108 North Greene Street, Baltimore, Maryland 21201.
[2] Department of Physiology, University of Maryland, School of Medicine, 660 West Redwood Street, Baltimore, Maryland 21201.
[3] Department of Pharmacology, University of Virginia School of Medicine, Room 448, Jordan Hall, Charlottesville, Virginia 22908.

1053-0509/93/0900-0161$07.00/0

aging circumvents the needs for wavelength-ratiometric probes. Fluorophores that display a change in lifetime, regardless of changes in the excitation or emission spectra, are perfectly suitable for FLIM.

The rapid time scale of fluorescence emission imposes significant constraints on the methods for measuring the decays. The emission typically occurs on the picosecond–nanosecond time scale and can be a single- or multiexponential decay. Due to the expense and complexity, time-resolved measurements are performed mostly as single-sample (single-pixel) measurements. Good accounts of such measurements are given elsewhere [9,10]. Very little attention has been paid to lifetime measurements microscopic samples [11,12]. The most recent advances in time-resolved fluorescence microscopy with two-dimensional (2-D) imaging of fluorescence lifetimes utilize high-speed 2-D images detectors. Several different detection systems for creation images based on the fluorescence lifetime have already been developed. A comprehensive review of some of currently developed FLIM techniques with respect to lifetime resolution, formation of 2-D images, and measurement time has been published recently [13].

INSTRUMENTATION AND METHODOLOGY FOR FLIM

The electronic components and gain-modulated image intensifier in our FLIM apparatus were described previously [14,15]. This method uses a fluorescence microscopy, high-speed gated proximity focused MCP image intensifier, and slow-scan CCD camera (Fig. 1). To accomplish subnanosecond time-resolved imaging, the gain of the image intensifier is modulated with a high-frequency signal that is synchronized with the intensity-modulated excitation. The voltage between the photocathode and the MCP input surface is varied at the desired frequency. The electronic gain is varied at a modulation frequency equal to the light modulation frequency or a harmonic of the pulse rate. This procedure results in a stationary phase-sensitive intensity image on the output screen of the image intensifier, which is recorded using a cooled slow-scan CCD camera and stored in an image processor. The lifetime images are created from a series of phase-sensitive images at various phase shifts on the gain modulation signal. This method of lifetime imaging has been evaluated using macroscopic samples where the data were compared with standard lifetime measurements [16,17].

Phase-Sensitive Image Detection

In our apparatus the two-dimensional sample is excited by the intensity-modulated laser light at circular frequency ω and modulation degree m_E. The sinusoidally modulated emitted fluorescence is phase-shifted and partially demodulated relative to the excitation. The phase angle, $\theta_F(r)$, and the fluorescence modulation degree, $m_F(r)$, depend on the lifetime at each position, r, and on the light modulation frequency,

$$\tan\theta_F(r) = \omega\tau_p(r), \quad m_F(r) = m_E\,[1+\omega^2\tau_m^2(r)]_2^{-1} \quad (1)$$

where $\tau_p(r)$ and $\tau_m(r)$ are apparent phase and modulation lifetimes at each position, r. For a single-exponential decay, the phase and modulation lifetimes are equal and independent of modulation frequency. Generally, the emission kinetics are more complicated, and the intensity decays are mostly multiexponential or nonexponential, especially in polymers and biological systems. For a multiexponential decay, generally $\tau_p < \tau_m$ and both of these apparent lifetimes decrease with an increase in modulation frequency.

The gain-modulation signal applied to the photocathode of the image intensifier results in a time-varying gain $G(t)$, with

$$G(t) = G_o\,[1 + m_D\sin(\omega t - \theta_D)] \quad (2)$$

where m_D is the gain-modulation degree, and θ_D is the detector phase angle relative to the excitation phase angle. The time-dependent photocurrent (intensity-modulated fluorescence) is multipled by the time dependent varying gain $G(t)$, resulting in a DC signal and high-frequency signals. However, due to the slow time response of the image intensifier screen ($\sim$1 ms), the high-frequency signals are averaged at the output screen. The time-averaged phase-sensitive intensity from the corresponding position, r, is given by

$$I(r,\theta_D) = I_o(r)\,[1+\frac{1}{2}m_D m(r)\cos(\theta(r)-\theta_D)] \quad (3)$$

The phase-sensitive intensity at each position r depends on the gain modulation of the detector m_D, the modulated amplitude of the emission $m(r)$, and the cosine of the phase-angle difference between the gain-modulation signal θ_D and the phase of the emission $\theta(r)$. The phase-sensitive intensity images are constant intensity at each position r, where the values depend on the concentration of the fluorophore $c(r)$ and lifetime $\tau(r)$. It is not possible to calculate the fluorescence phase angle $\theta(r)$ or modulation $m(r)$ images from a single phase-sensitive image. However, the phase angle and modulation of fluorescence can be determined from a series of phase-sensitive

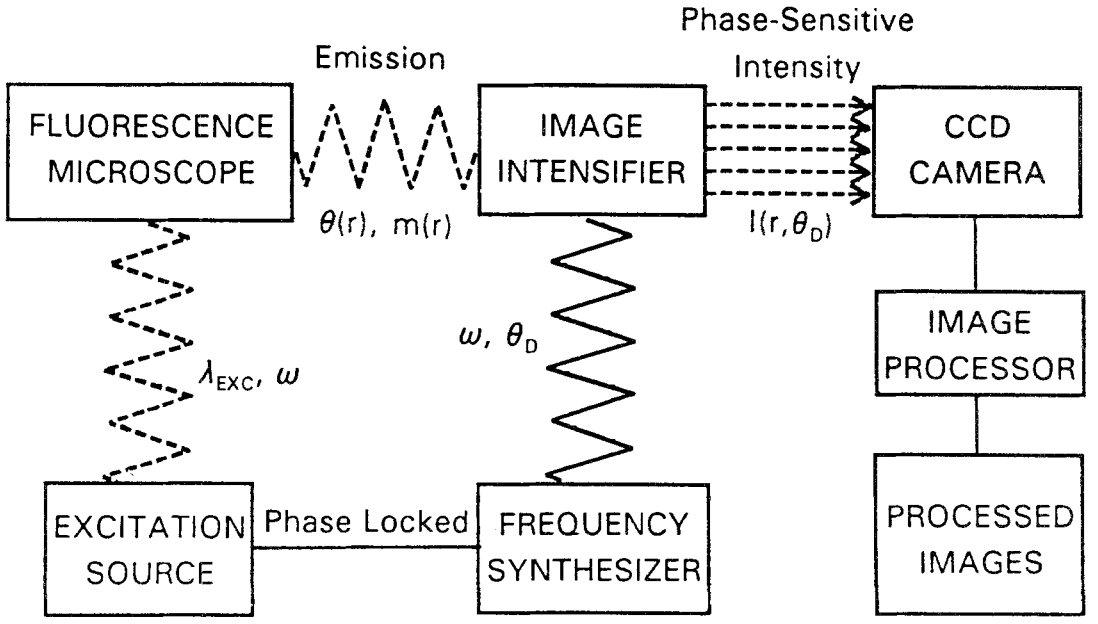

Fig. 1. Instrumentation for FLIM. The excitation is presently the frequency-doubled output of a pyridine-1 dye laser, which is synchronously pumped by a mode-locked Nd:YAG laser and cavity dumped at 3.81 MHz. The excitation light is expanded by a Newport LC075 (10×) laser beam expander. A Nikon Diaphot-TMD inverted fluorescence microscope is used, with Nikon Fluor 40×, NA 1.3, and DM400 Nikon dichroic beam splitter (DBS). The gated image intensifier (Varo 510-5772-310) is positioned between the target and the CCD camera. The gain of the image intensifier is modulated using the output of a PTS 300 synthesizer with a digital phase shift option. The detector is a CCD camera (Photometrics, Series 200, thermoelectrically cooled PM 512 CCD). The image processor is a 486DX/33MHz PC.

images by varying the phase angle of the detector, θ_D [Eq. (3)].

In our measurements we collect a series of phase-sensitive intensities in which θ_D is varied over 360°. Figure 2 shows a selected phase-sensitivity images of the Quin-2 in COS cells obtained using instrumentation described in Fig. 1. The phase-sensitive images in Fig. 2 contain the primary information about the decay time of the fluorescence at each position. These phase-sensitive intensities were used to compute the phase-angle and modulation images.

Phase and Modulation Images

The fluorescence phase angle is related to the detector phase θ_D, which includes a constant instrumental

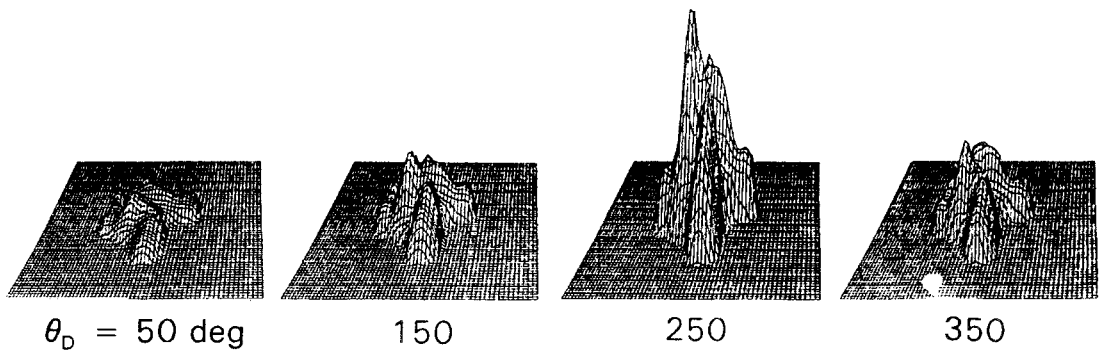

Fig. 2. Selected phase-sensitive intensity images of the fluorescence of Quin-2 within the COS cell obtained at a modulation frequency of 49.53 MHz, using instrumentation described in Fig. 1.

phase shift θ_I (electronic and optical pathways). Similarly, the fluorescence modulation is affected by instrumental modulation m_I. To determine the instrumental phase angle and modulation, which are need to calculate the apparent lifetimes [Eq. (1)], a reference sample is required, scattered light or fluorescence at a known phase and modulation. In our experiment we used the fluorescent standard DMSS (4-diethylamino-ω-methylsulfonyl-*trans*-styrene) in PVA film, which has a mean lifetime near 1 ns and an emission spectrum in the wavelength range of Quin-2 [16]. Reference phase-angle and modulation images are necessary to correct for a constant instrumental phase shift θ_I and modulation m_I and for the nonideal response of the image intensifier.

Figure 3 shows a plot of the averaged phase-sensitive intensities versus the detector phase angle visualizing the phase angle and modulation of Quin-2 relative to the reference sample. For these plots, averaged intensities were obtained for 5 × 5 pixels, using the same spatial window for all data files (Quin-2 and reference). The apparent phase angles and modulations are included in Fig. 3. The instrumental phase shift θ_I = 196.5°) and modulation (m = 0.52) were calculated using known values for DMSS (θ_R = 20.0°) and m_R = 0.90 at 49.335 MHz) [15] and its apparent values (216.5° and 0.47, respectively). The phase-angle and modulation corrections with respect to the nonideal spatial response of image the intensifier are described elsewhere [15].

One can imagine that such calculations are performed on each pixel. The data sets for FLIM are rather large (in our case, 512 × 512 pixels, resulting in about 520 kbyte storage per each image), which can result in time-consuming data storage, retrieval, and processing. To allow rapid calculation of images we developed an algorithm that uses each phase-sensitive image only one time. The task is to use a set of images taken at different detector phase angles (Fig. 2) and generate three images. The first of these desired images is of the phase of the fluorescence, $\theta(r)$, in Eq. (3). The second is an image of the modulated amplitude of the fluorescence at a particular detector modulation frequency [i.e., the AC component or $m(r)$ in Eq. (3)]. The third is an image of the steady-state or DC component of the fluorescence. To allow rapid calculations of images, an algorithm has been developed that uses a linearized version of Eq. 3 [16].

RESULTS

Intracellular Calcium Concentration Imaging

We used COS cells (from green monkey kidney epithelium) to work out the technical requirements for

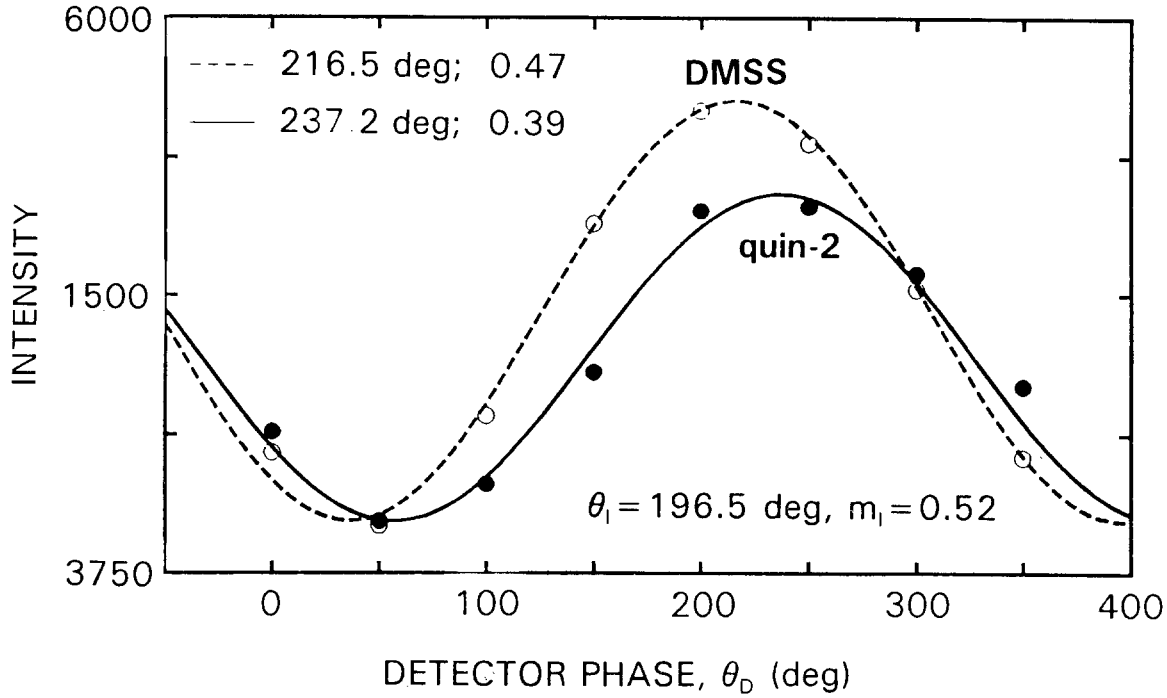

Fig. 3. Plots of the averaged phase-sensitive intensities for Quin-2 in the COS cell (——) and for DMSS in PVA film as a reference) (—).

FLIM imaging in a cellular system. COS cells were selected for these experiments because they are relatively flat in terms of their biological architecture, easy to grow, and adhere moderately well to the glass surface. The cells were loaded with the calcium probe Quin-2 by exposure to Quin-2 AM. The fluorescence lifetime of Quin-2 is strongly dependent on Ca^{2+} [18–20]. The calcium-induced change in the lifetime of Quin-2 results in a dramatic change in phase angle and modulation versus free calcium concentration in the range from 0 to 600 n*M* [18]. Phase-sensitive images were collected using instrumentation described in Fig. 1 at a modulation frequency of 49.53 MHz.

Figure 4A shows that the local intensity varies dramatically throughout the cell. The phase-angle and modulation images (Figs. 4B and C, respectively) display relatively constant values throughout the cell (average values, 38.0° for phase angle and 0.74 for modulation from about 80% of the cell), suggesting that the Ca^{2+} concentration is uniform. This result demonstrates not only the relatively uniform concentration of calcium in the cell, but also the ability of the FLIM method to provide reliable lifetime images over a wide range of probe concentration and/or intensities. This constancy is in agreement with the result of ratiometric imaging in comparable cells [21].

Transformation of a phase-angle and/or modulation image into a $[Ca^{2+}]$ image requires calibration curves. The calibration curves were determined from phase and modulation measurements of Quin-2 in cuvettes using EGTA/Ca-calibrated buffers under the same conditions used for cellular imaging. Ca^{2+}-dependent phase-angle values of Quin-2 at 49.335 MHz (Fig. 5) were used to transform phase-angle image into the $[Ca^{2+}]$ image. The average value of the Ca^{2+} concentration for the central 80% of the cell is 16.7 ± 2.3 n*M*. This apparent $[Ca^{2+}]$ is in agreement with other measurements using Quin-2 [22–24]. However, the expected concentration is higher than 100 n*M*, and such higher values are usually observed with Fura-2 or Indo-1. Also, significant discrep-

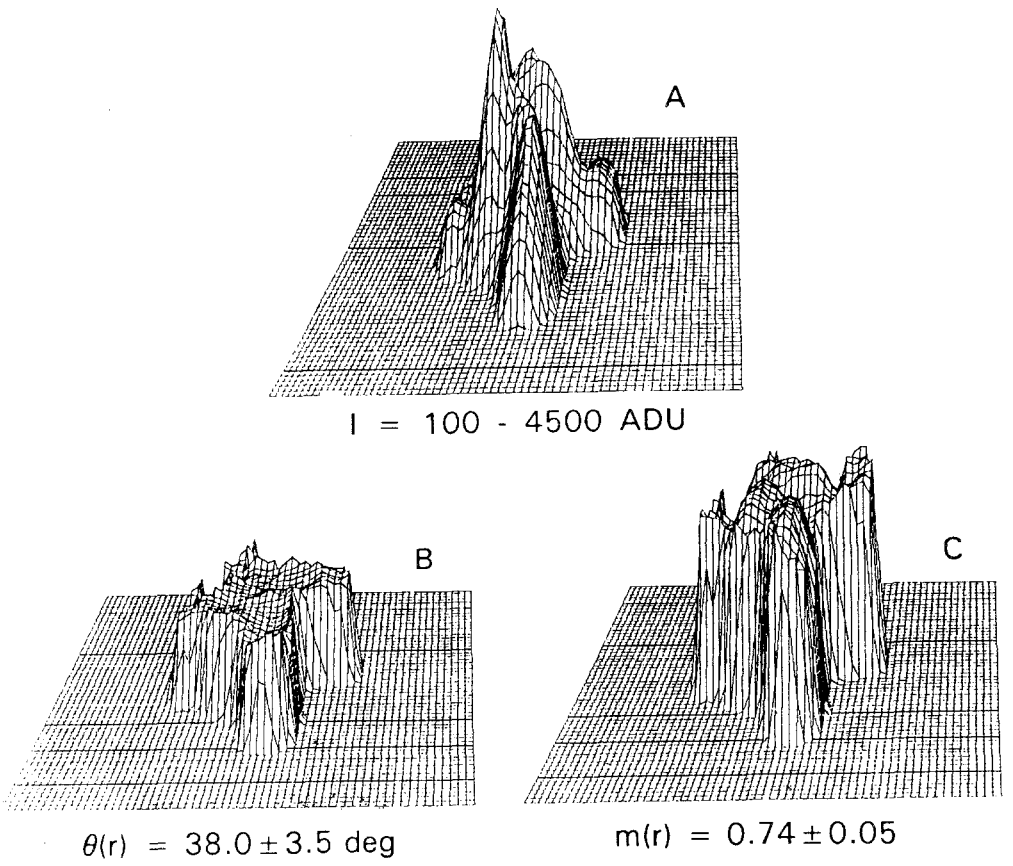

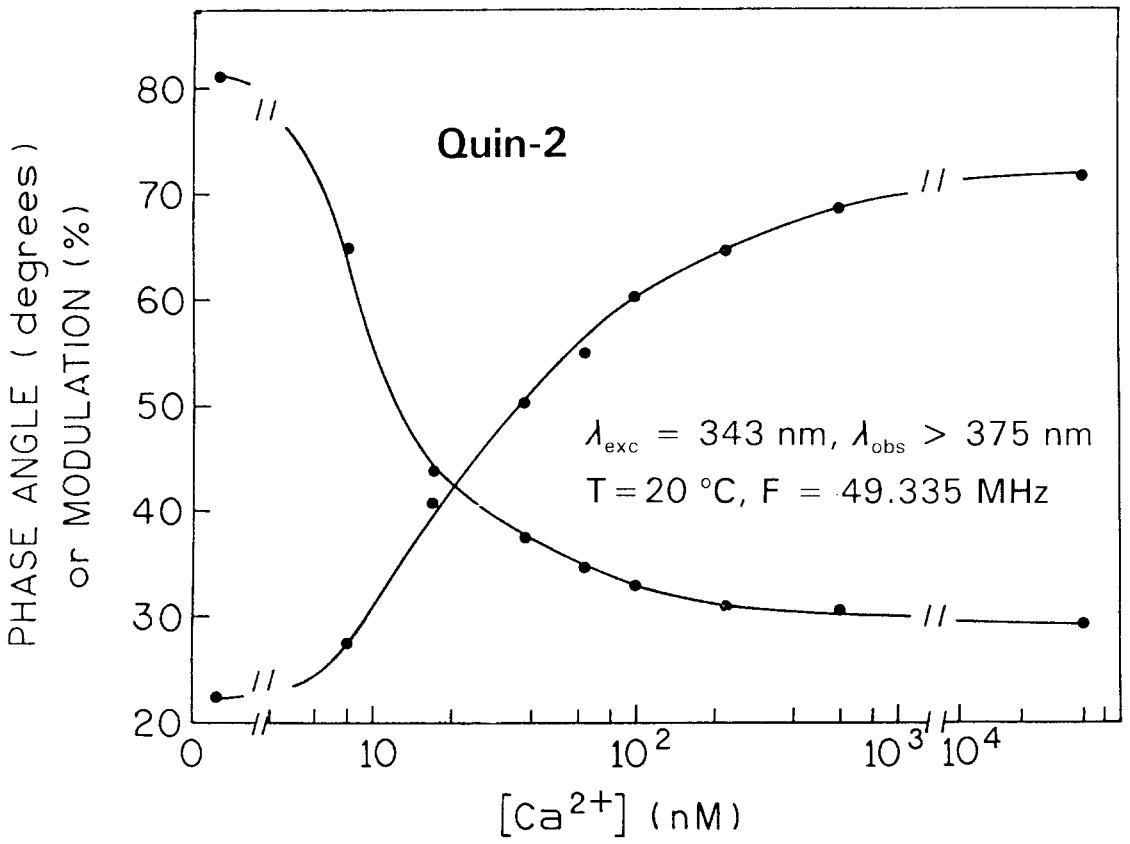

Fig. 5. Phase and modulation calibration curves for Quin-2 obtained using calibrated Ca/EGTA buffers (100 m*M* KCl, 10 m*M* MOPS, 0–10 m*M* Ca EGTA, pH 7.2).

ancies in the measured cytosolic free Ca^{2+} concentrations were observed with various methods, and Quin-2 yielded the lowest $[Ca^{2+}]$ [25]. These led us to question whether Quin-2 was forming fluorescent photoproducts during illumination of the labeled cells. We have found that, with the extent of illumination, the phase angle and modulation changed continually, which indicates the formation of fluorescent photoproducts. A multiexponential analysis of intensity decays of Quin-2 before and after photobeaching and its effect on calibration curves are presented elsewhere [15]. The average Ca^{2+} concentration determined for this cell using the phase-angle calibration curve after about 60% of photobleaching is 155 ± 36 n*M*. Based on these results, it is essential that the Ca^{2+} probes be examined for phototransformation effects, whether the $[Ca^{2+}]$ values are determined by FLIM or wavelength-ratiometric methods. More detailed information on these cellular imaging experiments has been reported elsewhere [15].

SUMMARY

We demonstrated imaging of intracellular Ca^{2+} using our approach to FLIM. The ability to obtain calcium images using Quin-2 suggests that the method will be useful for many types of chemical imaging. The lifetime measurements and multiexponential analysis can reveal whether the probes photobleach, which will not cause a change in lifetime, or undergo transformation to fluorescent products, which will alter the calibration curves. We note that even the most widely used probe, Fura-2, has been reported to undergo phototransformation to species that are not sensitive to Ca^{2+} [26].

We know that the lifetimes of other probes are sensitive to analytes of interest. For instance, it is possible to use the nonratiometric probes calcium green, orange, and crimson [27] for lifetime imaging of Ca^{2+} using visible wavelength excitation and emission. The dual wavelength-ratiometric pH probes of the SNAFL and

SNARF series display pH-dependent lifetimes, and the apparent pK_a can be shifted by 4 pH units by selection of the emission wavelengths [28]. There are also chloride probes such as SPQ and MQAE based on collisional quenching [29], and Mg^{2+} can be imaged using magnesium green [30], Mag-Quin-2, and Mag-Quin-1 [31]. Hence, FLIM offers many opportunities for chemical imaging of cells.

ACKNOWLEDGMENTS

This work was supported by National Institute of Health (NIH) Grant RR-08119, with additional support from NIH Grant RR007510 and from National Science Foundation Grant DIR-8710401.

REFERENCES

1. Y. Wang and D. L. Taylor (Eds.) (1989) *Fluorescence Microscopy of Living Cells and Culture, Part A. Fluorescent Analogues, Labelling Cells, and Basic Microscopy*, Academic Press, New York.
2. D. L. Taylor and Y. Wang (Eds.) (1989) *Fluorescence Microscopy of Living Cells and Culture, Part B. Quantitative Analogues, Microscopy-Imaging and Spectroscopy*, Academic Press, New York.
3. S. Inoune (1989) *Video Microscopy*, Plenum Press, New York.
4. B. Herman and K. Jacobson (Eds.) (1990) *Optical Microscopy for Biology,* Wiley-Liss, New York.
5. E. Kohen, J. S. Ploem, and J. G. Hirschberg (Eds.) (1989) *Cell Structure and Function by Microspectrofluorometry*. Academic Press, New York.
6. J. Cherry (Ed.) (1991) *New Techniques in Optical Microscopy and Spectrometry*, Macmillan, London.
7. R. P. Haugland (1992–1994) *Molecular Probes. Handbook of Fluorescent Probes and Research Chemicals*, Molecular Probes, Inc., Eugene, OR.
8. *Bioprobes 17* (June 1993), Molecular Probes, Inc., Eugene, OR.
9. J. R. Lakowicz (1983) *Principles of Fluorescence Spectroscopy*, Plenum Press, New York.
10. J. N. Demas (1983) *Excited State Lifetime Measurements*, Academic Press, New York.
11. H. Scheckenburger, H. K. Seidlitz, and J. Eberz (1988) *J. Photochem. Photobiol. B Biol* **2,** 1–19.
12. R. Tian, M. A. J. Rodgers, and J. Cherry (Ed.) (1991) *New Techniques in Optical Microscopy and Spectrophotometry*, Macmillan, London, pp. 177–179.
13. X. F. Wang, A. Periasamy, B. Herman, and D. M. Coleman (1992) *Anal. Chem.* **23,** 369–395.
14. J. R. Lakowicz and K. W. Berndt (1991) *Rev. Sci. Instrum.* **67,** 1727–1734.
15. J. R. Lakowicz, H. Szmacinski, K. Nowaczyk, W. J. Lederer, M. S. Kirby, and M. L. Johnson (1994) *Cell Calcium* **15,** 7–27.
16. J. R. Lakowicz, H. Szmacinski, K. Nowaczyk, K. W. Berndt, and M. L. Johnson (1992) *Anal. Biochem.* **202,** 316–330.
17. J. R. Lakowicz, H. Szmacinski, K. Nowaczyk, and M. L. Johnson (1992) *Proc. Natl. Acad. Sci. USA* **89,** 1271–1275.
18. J. R. Lakowicz, H. Szmacinski, K. Nowaczyk, and M. L. Johnson (1992) *Cell Calcium* **13,** 131–147.
19. N. Miyoshi, K. Hara, S. Kimura, K. Nakanishi, and M. Fukuda (1991) *Photochem. Photobiol.* **53,** 415–418.
20. K. M. Hirshfield, D. Toptygin, B. S. Packard, and L. Brand (1993) *Anal. Biochem.* **209,** 209–218.
21. J. R. Berlin, M. A. Wozniak, M. B. Cannel, R. J. Bloch, and W. J. Lederer (1990) *Cell Calcium* **11,** 371–384.
22. B. A. Kruskal, C. H. Keith, and F. R. Maxfield (1984) *J. Cell Biol.* **99,** 1167–1172.
23. M. Rhoda, F. Giraud, C. Craescu, and Y. Beuzard (1985) *Cell Calcium* **6,** 397–411.
24. R. L. Waller, L. R. Johnson, W. J. Brattin, and D. G. Dearborn (1985) *Cell Calcium* **6,** 245–264.
25. M. David-Dufilho, T. Montenay-Garestier, and M.-A. Devynck (1988) *Cell Calcium* **9,** 167–179.
26. P. L. Becker and F. S. Fay (1987) *Am. J. Physiol.* **253,** C613–C618.
27. J. R. Lakowicz, H. Szmacinski, and M. L. Johnson (1992) *J. Fluoresc* **2,** 47–62.
28. H. Szmacinski and J. R. Lakowicz (1993) *Anal. Chem.* **65,** 1668–1674.
29. A. S. Verkman (1990) *Am. J. Physiol.* **259,** C375–C388.
30. H. Szmacinski and J. R. Lakowicz (1993) *Biophys. J.* **64,** A108.
31. H. Szmacinski and J. R. Lakowicz, unpublished observations.